RESEARCH ARTICLE | MAY 05 2020

Dissociative electron attachment to benzoic acid ($C_7H_6O_2$)

M. Zawadzki ; P. Wierzbicka ; J. Kopyra

J. Chem. Phys. 152, 174304 (2020)
https://doi.org/10.1063/1.5135383

The Journal of Chemical Physics ARTICLE scitation.org/journal/jcp

Dissociative electron attachment to benzoic acid ($C_7H_6O_2$)

Cite as: J. Chem. Phys. 152, 174304 (2020); doi: 10.1063/1.5135383
Submitted: 8 November 2019 • Accepted: 12 April 2020 •
Published Online: 5 May 2020

M. Zawadzki,[1,a)] P. Wierzbicka,[2] and J. Kopyra[2]

AFFILIATIONS

[1] Department of Atomic, Molecular and Optical Physics, Faculty of Applied Physics and Mathematics, Gdańsk University of Technology, ul. Gabriela Narutowicza 11/12, 80-233 Gdańsk, Poland
[2] Faculty of Exact and Natural Sciences, Siedlce University of Natural Sciences and Humanities, 3 Maja 54, 08-110 Siedlce, Poland

[a)] **Author to whom correspondence should be addressed:** mateusz.zawadzki@pg.edu.pl

ABSTRACT

The dissociative electron attachment (DEA) to benzoic acid (C_6H_5COOH) has been studied using an experimental crossed beam setup of a quadrupole mass spectrometer and a trochoidal electron monochromator. Relative partial cross sections for the DEA to produce negative ion fragments show the main channels for dissociation. The comparison of the present results with the ultraviolet photoelectron spectrum of benzoic acid [J. Meeks, A. Wahlborg, and S. P. McGlynn, J. Electron Spectrosc. Relat. Phenom. **22**, 43 (1981)] implies that most DEA bands in the high energy range are due to Feshbach resonances with double occupation of diffuse Rydberg-like orbitals. The measurements are supported by density functional theory calculations of the threshold energies.

I. INTRODUCTION

There have been many theoretical and experimental studies on the physico-chemical processes of the molecular complexes containing heterocyclic ring structures.[1–4] Such compounds have salient applications in interdisciplinary research, including biology, chemistry, medicine, pharmacology, and material science.[5–7]

It has been shown that adding large molecular structures to a ring molecule (e.g., uracil or furan) significantly affects its fragmentation when impacted by energetic electrons. Such fragmentation mechanisms are important in the case of secondary electrons induced by high energy radiation incident on biological tissues, which impact polyatomic tissue molecules and are responsible for reductive DNA strand breaks[8,9] caused by dissociative electron attachment (DEA) processes.

Benzoic acid (BA) is a compound comprising a benzene ring core carrying a carboxylic group, which categorizes this molecule as a simple aromatic carboxylic acid. BA is a colorless crystalline solid which can be synthesized by selective oxidation of benzyl alcohol with iron(III) and hydrogen peroxide.[10] Due to its capability of inhibiting, retarding, or arresting the process of fermentation, acidification, or other deterioration of foods, BA is popular as a food preservative; hence, this compound can be found in many food products.[11,12] In the pharmacological industry, BA is used as an antifungal agent.[13] From the physico-chemical point of view, this compound acts as a quencher of luminescent molecules[14] and is known to form dimers by hydrogen bonding.[15] BA was detected by the Rosetta Orbiter Spectrometer for Ion and Neutral Analysis (ROSINA) during the Rosetta mission. This aromatic ring compound was measured *in situ* during the monitoring of the 67P/Churyumov–Gerasimenko comet.[16]

Presently, in the literature, there is a paucity of experimental electron scattering studies with BA, likely because of its low volatility and hence the difficulty of handling experimentally. Among a few reports on electron interaction with BA, one can find studies on molecular structures of BA obtained by gas-phase electron diffraction and theoretical calculations.[17] Orientation and bonding of BA have been studied by high resolution electron energy loss spectroscopy (HREELS).[18]

In this paper, we present relative partial cross sections for individual DEA channels in BA. We report on five, the most dominant, dissociative channels revealing distinctive resonance structures. The measurements are supported by density functional theory (DFT) calculations of the asymptotic energetics, mainly the threshold energies. We also compare our results with the ultraviolet

photoelectron spectroscopy (PES) data along with a theoretical simulation by the composite molecule method (CMM) from the work of Meeks *et al.*[19]

II. EXPERIMENTAL

The experimental results were obtained in the Siedlce laboratory using a crossed electron-molecular beam apparatus. The vacuum chamber was equipped with an electron source, an oven, and a quadrupole mass analyzer (QMA). The components were housed in a UHV chamber at a base pressure of ≈3×10^{-8} mbar. A well-defined electron beam was generated from a trochoidal electron monochromator (≈220 meV FWHM and an electron current of 10–15 nA) and orthogonally intersected with an effusive molecular beam of benzoic acid. The molecular beam emanated from a vessel heated by two *in vacuo* halogen bulbs. The powder was heated up to 330 K, as measured by a platinum resistance mounted at one of the flanges. Since our experimental temperature was below the melting temperature (394–396 K), the evaporated molecules were likely to remain intact. Negative ions were generated in the reaction area due to the collision of electrons with intact molecules, extracted from the interaction area toward the QMA, and detected by single-pulse counting techniques. The intensity of negative ions was recorded as a function of the electron energy. The electron energy scale was calibrated by using the SF_6 gas yielding the well-known SF_6^- resonance near 0 eV. The width of the resonance was used for the determination of the electron energy resolution of the electron beam and its position to define the zero energy point of the energy scale. However, the measurements were performed without the presence of the calibration gas in order to avoid unwanted reactions of dissociative electron transfer. The sample of benzoic acid was purchased from Sigma Aldrich with a stated purity of 99.5% and was used without any further purification.

III. THEORETICAL METHODS

The present experimental work is supported with quantum chemical calculations of the bound electronic states. This approach provides a reliable location of threshold energy estimates for the dissociative electron attachment reactions in carbon-containing molecules.[20–24] Individual threshold energy calculations of the dissociative attachment scheme were based on the simple formula [related to Eq. (2)],[25,26]

$$E_{\mathrm{th}} = E_{\mathrm{M_a^-}} + E_{\mathrm{M_b}} - E_{\mathrm{M}}, \tag{1}$$

where $E_{\mathrm{M_a^-}}$ and $E_{\mathrm{M_b}}$ are the energies of the breakup products in the DEA process—for a newly formed stable negative ion and its neutral counterpart, respectively. E_{M} is the energy of the neutral parent molecule. This simple method can provide information on resonance energies and enable one to trace possible reaction pathways. Individual threshold energies are obtained from the sums of electronic and zero-point energies. All quantum-mechanical calculations were performed with the Gaussian 09 software.[27] The atoms were described by the standard aug-cc-PVTZ basis set, whereas DFT calculations for BA geometries optimization used the hybrid B3LYP method[28,29] where open shell systems are treated with the unrestricted approach by default.

IV. RESULTS AND DISCUSSION

Considering the orientation of the hydrogen atom from the carboxylic part with respect to the ring structure one can distinguish two conformers of BA (see Fig. 1). The calculated relative energy levels between these two conformers differ by 0.26 eV. In Sec. IV, we present experimental results of the DEA to BA and its calculated threshold energies. In these DEA threshold calculations, we use the lowest energy conformer A of BA.

In general, the DEA to the BA molecule is a process that can be represented by the following equation:

$$e^- + \underbrace{C_6H_5COOH}_{M=M_a+M_b} \overset{M^{\#-}}{\rightarrow} M_a^- + M_b, \tag{2}$$

where we can distinguish the creation of a transient parent anion $M^{\#-}$ of target molecule M and then the fragmentation into a detected negative fragment ion M_a^- and one (or more) undetected neutral fragment M_b. Our present experiment reveals five main dissociation channels from gas-phase BA, namely, $(M–H)^-$, $C_6H_5^-$, OH^-, $COOH^-$, and O^-. All of them are generated from the deterioration of the exocyclic group of the BA, while the benzene ring stays intact.

In Fig. 2, we present the ion yield curves for the formation of different negative ions due to the dissociative electron attachment process. All ion yields display the expectedly pronounced resonance profiles, with the relative scale arranged in decreasing intensity order. In the same figure, the values of calculated threshold energies (E_{th}) for individual dissociation channels are also indicated next to the ion yields to enable comparison of theoretical evaluations of the resonance onsets. Table I presents the threshold energies obtained from the sums of electronic and zero-point energies for each DEA channel. We note that individual resonances peak at somewhat different electron energies, but in general, we can distinguish several distinctive energy bands centered around 1.34 and 5.7, possibly two overlapping bands at 6.7 and 7.2, and a broader, multi-resonance feature centered between 8 eV and 10 eV, which are visible in Fig. 2.

The most copiously generated ion forms the band centered at 1.34 eV. It is related to a dehydrogenated closed-shell anion $(M–H)^-$. This fragment is formed by the loss of a neutral hydrogen

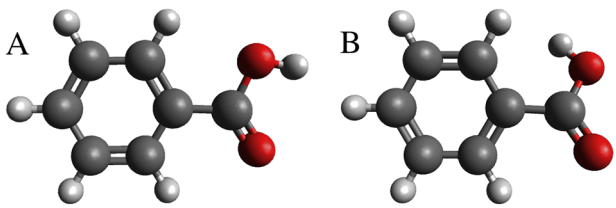

FIG. 1. Optimized molecular structures of two monomeric conformers of BA. DFT calculations for BA geometries optimization used the hybrid B3LYP method and the standard aug-cc-PVTZ basis set. The calculated energy difference (the sum of electronic and zero-point energies) between the molecular structure on the left (conformer A) and the molecular structure on the right (conformer B) is 0.26 eV.

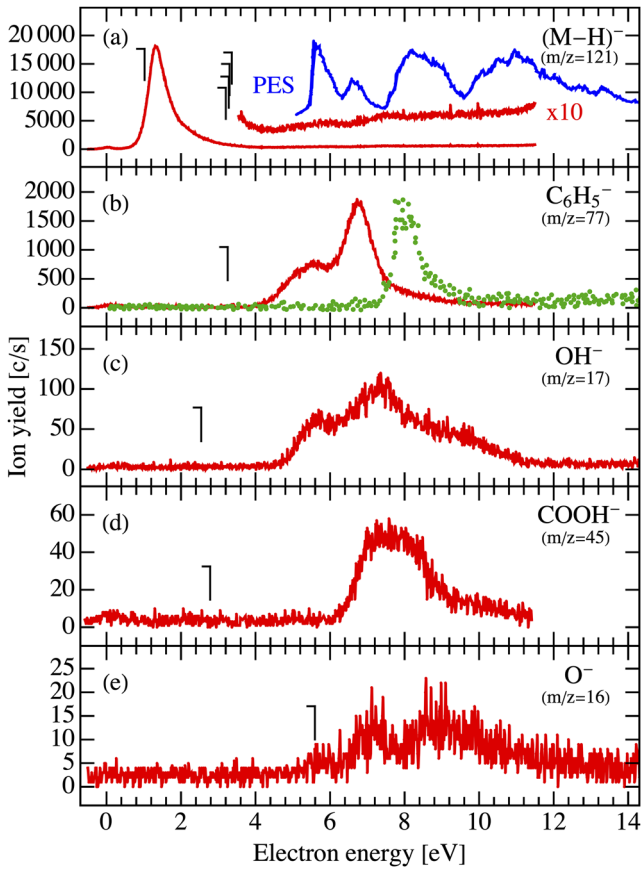

FIG. 2. Ion yields [(a)–(e)] for individual DEA fragments of BA acid with the calculated threshold energies (from Table I) for individual dissociation channels. The top (blue) trace represents PES spectrum from Ref. 19 for comparison. Ion yields (b) for the formation of $C_6H_5^-$ (green dots) are the data points from Ref. 22 (see the text for discussion).

atom leading to a stable anion as (with its indicated ring and carboxyl parts)

$$e^- + \overbrace{\underbrace{C_6H_5}_{\text{ring}}\,\underbrace{COOH}_{\text{carboxyl}}}^{\text{M}} \xrightarrow{M^{\#-}} \underbrace{(C_6H_5\,COO)^-}_{(\text{M-H})^-} + H. \qquad (3)$$

This channel is to be found in many organic and biological complexes.[20,30,31] In the BA molecule, there are six hydrogen atoms that can cleave from the parent molecule. Five of them are directly attached to the benzene ring and one hydrogen at the carboxylic part of the molecule. Employing our threshold energy calculations we can deduce which hydrogens contribute to the ion yield signal. Only the hydrogen from the carboxylic group fulfills the energy onset requirement (see Table I). Comparing the present results with those obtained from DEA to formic acid,[32] it appears that there is a very good agreement of the resonance position, which confirms that the hydrogen atom is detached from the carboxylic group. In addition, we have performed the DFT calculations to obtain the adiabatic electron affinity (EA) of the (M–H) radical. It appeared that the

TABLE I. B3LYP/aug-cc-pVTZ threshold energies for BA DEA channels.

Dissociation scheme	Anion	Products	*m/z*	E_{th} (eV)
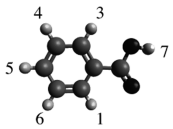	$(M\text{-}H_i)^-$	$+ H_i$	121	
		$+ H_1$		3.36
		$+ H_3$		3.28
		$+ H_4$		3.28
		$+ H_5$		3.20
		$+ H_6$		3.30
		$+ H_7$		1.02
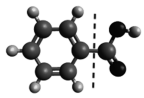	$C_6H_5^-$	+ COOH	77	3.25
		$+ CO_2 + H$		3.31
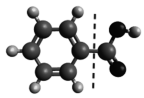	$COOH^-$	$+ C_6H_5$	45	2.78
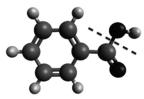	OH^-	$+ C_6H_5CO$	17	2.54
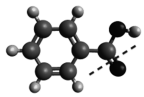	O^-	$+ C_6H_5COH$	16	5.59

EA = 3.43 eV of the (M–H) radical from BA is comparable with the EA of the HCOO radical from formic acid (3.50 eV[33]). The appreciable EA of (M–H) radicals allows the corresponding DEA reaction to take place at low energy range.

The ion yield of $(M–H)^-$ is the only one peaking at a lower energy range. The rest of the fragment anion resonances are centered above 5 eV. In general, these broader and overlapping features (>5 eV) can be characterized as core excited (Feshbach) resonances.[34] The energies of these Feshbach resonances exhibit a simple relation to the energies of the parent Rydberg states and the grandparent state of the cation.[35–38] The comparison of the present results with the ultraviolet photoelectron spectrum of benzoic acid implies that most DEA bands in the high energy range are due to Feshbach resonances with double occupation of diffuse Rydberg-like orbitals. In this energy range, we observe three further fragment anions generated from the decomposition of the exocyclic group, namely: $COOH^-$, OH^-, and O^-. While $COOH^-$ and OH^- can be formed from a simple bond rupture, the formation of the O^- anion requires the cleavage of a double C=O bond. The positions of the peaks within the ion yield curve of O^- nicely resemble those observed for formic acid.[32,39] On the other hand, the yield curve of OH^- is composed of three overlapping structures and only the middle structure, centered at around 7.5 eV, was previously observed from

HCOOH. Further fragment $COOH^-$ generated from cleavage of a single bond between the benzene ring and the exocyclic group is visible via a very broad structure between 6.5 eV and 9 eV with possible small contribution above 9.5 eV. In principle, the structural composition of the ion $COOH^-$ resemble that of the dehydrogenated ion ($HCOO^-$) generated from DEA to HCOOH. However, the resonance positions are very different. As mentioned, while DEA to BA to form $COOH^-$ is only visible at high energy domain, in formic acid, the fragment anion is generated exclusively at 1.3 eV. This must reflect the different mechanisms of the electron attachment process resulting in the formation of the fragment at m/z 45 from both compounds.

During the DEA process, the interacting electron causes the breakage of the covalent bond between a carboxylic part and a benzene ring. The interacting electron can attach to either the benzene ring or the carboxyl moiety. This results in two competitive dissociation channels, producing $C_6H_5^-$ or $COOH^-$ anions at around 6.9 eV. A similar scenario was reported by Ptasinska *et al.*[40] in the case of thymidine. A rupture of the glycosidic bond between the thymine and the ribose moiety was caused by the interacting electron. The resonant features associated with the breakage of this bond were observed through the thymine and the sugar moiety anions. In the case of BA, by integrating the individual ion yield signal for these fragmentation channels ($C_6H_5^-$ and $COOH^-$), we can estimate the branching ratio of the observed ion. This estimation shows that electrons are most likely attached to the benzene ring moiety (96%) creating $C_6H_5^-$ in the dissociation process with respect to the possible creation of the $COOH^-$ anion (4%). The benzene ring acts as a strong base, which is favorable for attachment of the incoming electron.

We also would like to compare the $C_6H_5^-$ negative ion signal that originates from two different molecular targets. The $C_6H_5^-$ ions from our present experiment originate from the cleavage of the carboxylic part of the molecule, COOH (see Table I). The resulting molecular structure is in the form of the benzene ring without one hydrogen. The same negative ion molecular structure was recorded by Fenzlaff and Illenberger[22] when they measured the DEA signal from benzene itself. The prominent DEA signal for benzene ($(M\text{-}H)^-_{benzene} \equiv C_6H_5^-$) is shown in Fig. 2(b) with the same anionic fragment originating from BA. We normalized the signal from Ref. 22 for a clearer comparison. In the case of $C_6H_5^-$ from benzene, one can see a pronounced peak around 8 eV with a smooth decaying right-side wing. A similar structure is demonstrated by our present results, but it is shifted by ≈1.3 eV towards the lower energy. A very similar energy shift is seen when comparing PES spectra for benzoic[19] acid and benzene,[41] between the PES spectrum band related to the n MO in benzoic acid placed at 10.6 eV and PES features that represent $3e_{2g}$ orbitals of benzene, which are spanned around 12 eV.

Interestingly, when the energy bands from our present work is compared with the PES data and with a theoretical composite molecule method (CMM) calculations for BA,[19] we can observe relationships between them. The energetics of the Feshbach resonances can be compared with the energetics of the PES, with a notable energy difference of usually a few eVs between them, due to the formation of the Rydberg state and stabilization energy.[42,43] The PES from the study of Meeks *et al.*[19] reveals distinct bands in the region of 9–18 eV. The first band predicted by the CMM is assigned to the π_1, π_2 molecular orbital (MO) and calculations place the resonances at 9.5 eV. The π_1, π_2 MO is the $e_{1g}\pi$ orbital of benzene, which splits into two components, π_1 and π_2, in benzoic acid. The next band related to the n MO is estimated by the CMM to peak at 10.3 eV. This structure is assigned to the nonbonding σ orbital on the carbonyl oxygen. Finally, the theoretical CMM simulation predicts the π_0 MO between 11.4 eV and 12.5 eV. The PES of benzoic acid displays these features at 9.6 eV (π_1, π_2), 10.6 eV (n), and 11.4 eV (π_0). DEA bands correspond to the distinctive PES features—see Table II. We use here the well-known relation between the grandparent cation, parent Rydberg state, and daughter Feshbach resonance.[35–38] The energy difference between corresponding DEA and PES bands can be estimated to be ≈3.9 eV. Typically, previous reports found the energy shift within the range of 3.3–4.5 eV depending on the molecular target.[4,20,43] By offsetting the PES energy scale, we can see a very good agreement between the present experimental data and PES signal from the work of Meeks *et al.*[19]

TABLE II. The assignment of the DEA bands to the PES results and CMM calculations from the work of Meeks *et al.*[19]

DEA (eV)	→	PES (eV)	CMM (eV)
5.7		9.6	9.5
6.7		10.6	10.3
7.2		11.4	11.4–12.5
8.0–10.0		11.9–12.9	

In Fig. 2 of Ref. 19, above the energy of 11.4 eV (π_0), two additional PES structures are shown, i.e., π_3 and σ. Unfortunately, there is no theoretical treatment of these bands in Ref. 19, but it can suggest that σ will couple with available π states, resulting in mixed resonances, leading to dissociation. It is especially possible as σ states are usually quite broad, even of the order of few eVs.

Also, Fig. 2 shows a distinctive band around 5.7 eV corresponding to the productions of the $C_6H_5^-$ and OH^-. Available PES data relate the band to the π_1 and π_2 MOs on the benzene ring. The appearance of this band for $C_6H_5^-$ and the OH^- can suggest that other possible mechanisms might be involved leading to dissociation, including conical intersection. When comparing the branching ratio (of the 5.7 eV band) for these two anionic parts, we conclude that the formation of $C_6H_5^-$ is around 15 times greater than OH^-.

V. CONCLUSIONS

In present work, we have measured dissociative electron attachment to BA. The DEA signals can be used as a guide in the controllable fragmentation of the BA molecule. As a result, a variety of negative ions have been revealed, with the strongest dissociation channel originating from the cleavage of the bond within the hydroxyl group—which leads to the production of the $(M\text{–}H)^-$ anion at electron energies around 1.34 eV. Another four distinctive energy bands were explored at 5.7, 6.7, 7.2, and around 8–10 eV. These molecular orbital resonances (>5 eV) give rise to four, most prominent, DEA products: $C_6H_5^-$, OH^-, $COOH^-$, and O^-. The comparison of the resonances of formic acid and BA, for m/z 45, suggests

different mechanisms of the electron attachment process. Our measurements, based on a different experimental technique, confirm the results of the ultraviolet photoelectron spectrum and theoretical composite molecule method calculations from the study of Meeks *et al.*[19] when comparing higher energy resonances. As an outlook, it would be interesting to perform advanced scattering calculations on the mechanism producing discovered DEA resonances.

ACKNOWLEDGMENTS

J.K. acknowledges support by a statutory activity subsidy (No. 277/S/11) from the Polish Ministry of Science and Higher Education. M.Z. acknowledges the Academic Computer Center in Gdańsk (TASK) for a computational grant and support from the National Science Center (Poland) research Grant No. 2018/02/X/ST2/01946.

REFERENCES

[1] J. D. Gorfinkiel and S. Ptasinska, J. Phys. B: At., Mol. Opt. Phys. **50**, 182001 (2017).
[2] Z. Li, I. Carmichael, and S. Ptasińska, Phys. Chem. Chem. Phys. **20**, 18271 (2018).
[3] J. Kočišek, A. Pysanenko, M. Fárník, and J. Fedor, J. Phys. Chem. Lett. **7**, 3401 (2016).
[4] R. Janečková, O. May, A. R. Milosavljević, and J. Fedor, Int. J. Mass Spectrom. **163**, 365 (2014).
[5] P. Köpf-Maier and D. Krahl, Chem.-Biol. Interact. **44**, 317 (1983).
[6] C. V. Christodoulou, A. G. Eliopoulos, L. S. Young, L. Hodgkins, D. R. Ferry, and D. J. Kerr, Br. J. Cancer **77**, 2088 (1998).
[7] J. Langer, M. Zawadzki, M. Fárník, J. Pinkas, J. Fedor, and J. Kočišek, Eur. Phys. J. D **72**, 112 (2018).
[8] B. Boudaiffa, P. Cloutier, D. Hunting, M. A. Huels, and L. Sanche, Science **287**, 1658 (2000).
[9] F. Martin, P. D. Burrow, Z. Cai, P. Cloutier, D. Hunting, and L. Sanche, Phys. Rev. Lett. **93**, 068101 (2004).
[10] Z. Yang, C. Yu, S. Wu, W. Zhang, W. Xue, and Z. Zeng, Catal. Lett. **148**, 3082 (2018).
[11] F. J. Mota, I. M. Ferreira, S. C. Cunha, M. Beatriz, and P. Oliveira, Food Chem. **82**, 469 (2003).
[12] M. Dzięcioł, A. Wodnicka, and E. Huzar, Ecol. Chem. Eng. A **19**, 451 (2012).
[13] *Handbook of Pharmaceutical Excipients*, 6th ed., edited by R. C. Rowe, P. J. Sheskey, and M. E. Quinn (Pharmaceutical Press, London, England, 2009), p. 61.
[14] T. Miwa and M. Koizumi, Bull. Chem. Soc. Jpn. **38**, 529 (1965).
[15] M. Ito, J. Mol. Spectrosc. **4**, 144 (1960).
[16] A. D. Morse and Q. H. S. Chan, ACS Earth Space Chem. **3**, 1773 (2019).
[17] K. Aarset, E. M. Page, and D. A. Rice, J. Phys. Chem. A **110**, 9014 (2006).
[18] B. G. Frederick, M. R. Ashton, N. V. Richardson, and T. S. Jones, Surf. Sci. **292**, 33 (1993).
[19] J. Meeks, A. Wahlborg, and S. P. McGlynn, J. Electron Spectrosc. Relat. Phenom. **22**, 43 (1981).
[20] M. Zawadzki, M. Ranković, J. Kočišek, and J. Fedor, Phys. Chem. Chem. Phys. **20**, 6838 (2018).
[21] R. Janečková, O. May, and J. Fedor, Phys. Rev. A **86**, 052702 (2012).
[22] H.-P. Fenzlaff and E. Illenberger, Int. J. Mass Spectrom. **59**, 185 (1984).
[23] R. Janečková, D. Kubala, O. May, J. Fedor, and M. Allan, Phys. Rev. Lett. **111**, 213201 (2013).
[24] F. Ferreira da Silva, M. T. do N. Varella, N. C. Jones, S. Vronning Hoffmann, S. Denifl, I. Bald, and J. Kopyra, Chemistry **25**, 5498 (2019).
[25] I. I. Fabrikant, S. Eden, N. J. Mason, and J. Fedor, Adv. At., Mol., Opt. Phys. **66**, 545 (2017).
[26] H. Hotop, M.-W. Rul, and I. I. Fabrikant, Phys. Scr. **110**, 22 (2004).
[27] M. J. Frisch, G. W. Trucks, H. B. Schlegel, G. E. Scuseria, M. A. Robb, J. R. Cheeseman, G. Scalmani, V. Barone, B. Mennucci, G. A. Petersson, H. Nakatsuji, M. Caricato, X. Li, H. P. Hratchian, A. F. Izmaylov, J. Bloino, G. Zheng, J. L. Sonnenberg, M. Hada, M. Ehara, K. Toyota, R. Fukuda, J. Hasegawa, M. Ishida, T. Nakajima, Y. Honda, O. Kitao, H. Nakai, T. Vreven, J. A. Montgomery, Jr., J. E. Peralta, F. Ogliaro, M. Bearpark, J. J. Heyd, E. Brothers, K. N. Kudin, V. N. Staroverov, R. Kobayashi, J. Normand, K. Raghavachari, A. Rendell, J. C. Burant, S. S. Iyengar, J. Tomasi, M. Cossi, N. Rega, J. M. Millam, M. Klene, J. E. Knox, J. B. Cross, V. Bakken, C. Adamo, J. Jaramillo, R. Gomperts, R. E. Stratmann, O. Yazyev, A. J. Austin, R. Cammi, C. Pomelli, J. W. Ochterski, R. L. Martin, K. Morokuma, V. G. Zakrzewski, G. A. Voth, P. Salvador, J. J. Dannenberg, S. Dapprich, A. D. Daniels, Ö. Farkas, J. B. Foresman, J. V. Ortiz, J. Cioslowski, and D. J. Fox, GAUSSIAN 09, Revision D.01, Gaussian, Inc., Wallingford, CT, 2009.
[28] A. D. Becke, Phys. Rev. A **38**, 3098 (1988).
[29] C. Lee, W. Yang, and R. G. Parr, Phys. Rev. B **37**, 785 (1988).
[30] J. Kopyra, C. König-Lehmann, E. Illenberger, J. Warneke, and P. Swiderek, Eur. Phys. J. D **70**, 140 (2016).
[31] I. Baccarelli, I. Bald, F. A. Gianturco, E. Illenberger, and J. Kopyra, Phys. Rep. **508**, 1 (2011).
[32] A. Pelc, W. Sailer, P. Scheier, N. J. Mason, and T. D. Märk, Eur. Phys. J. D **20**, 441 (2002).
[33] E. Garand, K. Klein, J. F. Stanton, J. Zhou, T. I. Yacovitch, and D. M. Neumark, J. Phys. Chem. A **114**, 1374 (2010).
[34] E. Illenberger and J. Momigny, in *Gaseous Molecular Ions*, edited by H. Baumgartel, E. U. Frank, and W. Grunbein (Steinkopff Verlag Darmstadt, 1992).
[35] L. Sanche and G. J. Schulz, Phys. Rev. A **5**, 1672 (1972).
[36] G. J. Schulz, Rev. Mod. Phys. **45**, 423 (1973).
[37] L. Sanche and G. J. Schulz, J. Chem. Phys. A **58**, 479 (1973).
[38] B. Ibănescu and M. Allan, Phys. Chem. Chem. Phys. **10**, 5232 (2008).
[39] V. S. Prabhudesai, D. Nandi, A. H. Kelkar, R. Parajuli, and E. Krishnakumar, Chem. Phys. Lett. **405**, 172 (2005).
[40] S. Ptasinska, S. Denifl, S. Gohlke, P. Scheier, E. Illenberger, and T. D. Märk, Angew. Chem., Int. Ed. **45**, 1893 (2006).
[41] A. W. Potts, W. C. Price, D. G. Streets, and T. A. Williams, Faraday Discuss. Chem. Soc. **54**, 168 (1972).
[42] D. Spence, J. Chem. Phys. **66**, 669 (1977).
[43] B. C. Ibănescu, O. May, A. Monney, and M. Allan, Phys. Chem. Chem. Phys. **9**, 3163 (2007).